Incoherent Deep Virtual Compton Scattering off ^{4}He using CLAS spectrometer

M. Hattawy,[1,2] R. Dupré,[1,2] N.A. Baltzell,[1,3] and K. Hafidi[1,*]

(The CLAS Collaboration)

[1]*Argonne National Laboratory, Argonne, Illinois 60439*
[2]*Institut de Physique Nucléaire, CNRS/IN2P3 and Université Paris Sud, Orsay, France*
[3]*Thomas Jefferson National Accelerator Facility, Newport News, Virginia 23606*
(Dated: February 9, 2017)

We report the incoherent beam-spin asymmetry measurement of deeply virtual Compton scattering (DVCS) off ^{4}He. The experiment used the 6 GeV electron beam from Jefferson Lab projected onto a ^{4}He target in the center of the CEBAF Large Acceptance Spectrometer (CLAS).

PACS numbers: Valid PACS appear here

The main access to GPDs is through the measurement of deep virtual Compton scattering (DVCS), i.e. the hard exclusive electroproduction of a real photon. While other processes are known to be sensitive to GPDs, the measurement of DVCS is considered the cleanest probe and has been the focus of a worldwide effort [10–21] involving several accelerator facilities such as Jefferson Lab (JLab), HERA and CERN. The vast majority of these measurements focused on the study of proton structure and allowed extraction of the tomography of the nucleon (for details on the formalism, see [22–27]).

The experiment E08-024 took place in Hall-B at JLab in 2009 using the nearly 100% duty factor, longitudinally polarized electron beam (83% polarization) at its full energy of 6.064 GeV. The data were collected over three months using a 6 atm gaseous ^{4}He target placed in the center of CLAS. For DVCS experiments, the CLAS baseline design [37] is supplemented with an inner calorimeter (IC) and a solenoid. The IC extends the photon detec-

FIG. 1: Representation of the leading-order, twist-2, handbag diagram of the incoherent DVCS process off ^{4}He.

tion acceptance of CLAS, which was originally from $15°$ to $45°$, to polar angles as low as $4°$. At these small angles the low-energy Møller electrons produced in the target form a very high rate background that is suppressed by a 5 Tesla solenoid placed around the target.

To identify incoherent DVCS events, we first select events where one electron, one proton, and at least one photon are detected in the final state. Electrons are identified by using fiducial cuts and requiring appropriate signals in all the sub-detectors of the baseline CLAS (drift chambers, Cherenkov counters, electromagnetic calorimeter, and time of flight scintillators). Protons were identified with fiducial and timing cuts using the CLAS drift chambers and time of flight scintillators. In addition, we apply a vertex matching cut to ensure the electron and the proton originate from the same position. The photons are detected in either the IC or the CLAS electromagnetic calorimeter. Note that even though the DVCS reaction has only one real photon in the final state, events with more than one good photon are not discarded at this stage. This is motivated by the fact that, while soft photons are likely to be produced in random coincidence, they cannot be mistaken for the large energy DVCS photons (> 2 GeV). The most energetic photon is always considered as the DVCS photon candidate.

The main background in the measurement of DVCS is incoherent π^0 production. Therefore, we remove events where a π^0 can be identified by invariant mass reconstruction of two photons. To ensure the interaction occurs at the partonic level and the DVCS handbag diagram is dominant, we select events with $Q^2 > 1$ $[GeV^2/c^2]$. The exclusivity of the events is obtained by applying a set of cuts on the following kinematic variables: the co-planarity angle ($\Delta\phi$), the missing energy, the missing mass squared, the missing transverse momentum, the missing mass squared of the e'^4He' system, and the angle (θ) between the measured photon and the missing momentum of the e'^4He' system. The cuts are presented in Figure 2, which shows 3σ cuts except for the missing. After these requirements, we have about 20k events left, and Figure 3 presents their kinematic distributions
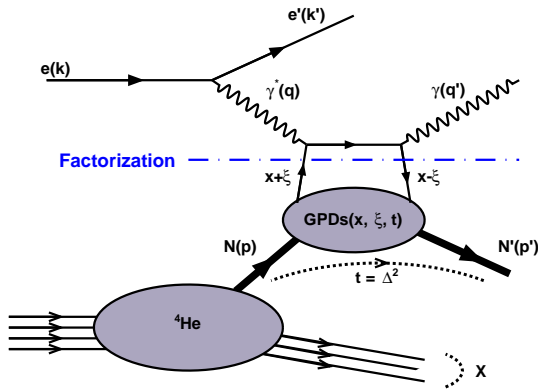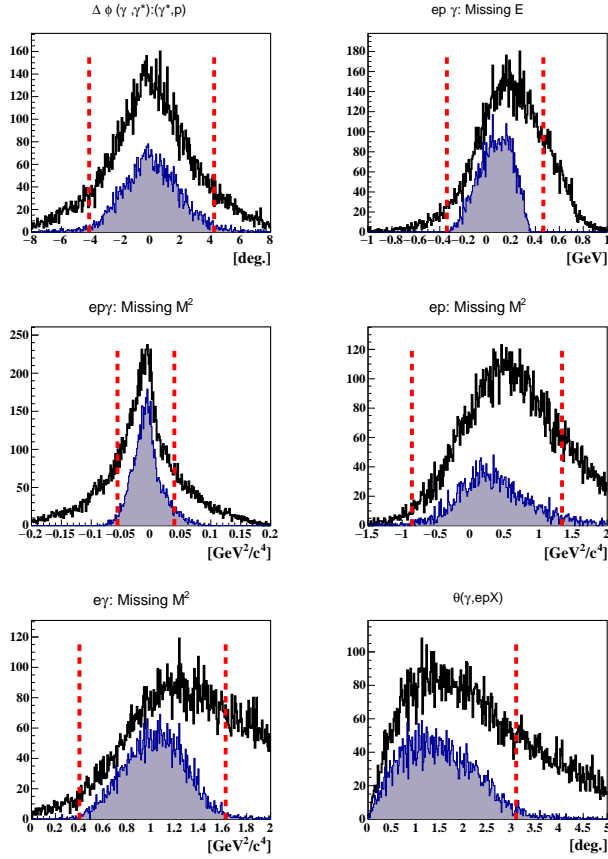
FIG. 2: The incoherent DVCS exclusivity cuts. The black distributions represent the coherent DVCS events candidate. The shaded distributions represent the events which passed all the exclusivity cuts except the quantity plotted. The vertical red lines represent the applied exclusivity cuts. The distributions from left to right and from top to bottoms are: $\Delta\phi$, missing energy, missing masses squared and the cone angle (θ) between the measured and the calculated photons.

in (Q^2, x_B) and $(Q^2, -t)$.

Several observables related to DVCS are of interest, but in this work we focus only on the beam-spin asymmetry. This observable is measurable using a polarized lepton beam on an unpolarized target (U). It is convenient to use the beam-spin asymmetry because most of the experimental normalization and acceptance issues cancel out in the asymmetry ratio. It is defined in terms of the cross sections as:

$$A_{LU} = \frac{d^5\sigma^+ - d^5\sigma^-}{d^5\sigma^+ + d^5\sigma^-}. \quad (1)$$

where $d^5\sigma^{+(-)}$ is the DVCS differential cross section for a positive (negative) beam helicity. Experimentally, A_{LU} can be expressed in terms of the measured number of events in each beam-helicity state (N^+, N^-) as:

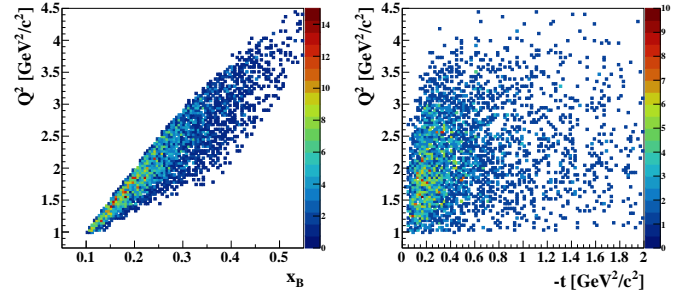$$A_{LU} = \frac{1}{P_B}\frac{N^+ - N^-}{N^+ + N^-}. \quad (2)$$

FIG. 3: Incoherent DVCS event distributions for Q^2 as a function of x_B (left) and Q^2 as a function of $-t$ (right) after the exclusivity cuts.

where P_B is the beam polarization, and N^+ and N^- are the number of DVCS events detected with positive and negative electron helicity with respect to the beam direction.

To interpret DVCS, one has to keep in mind that this reaction is indistinguishable from the Bethe-Heitler (BH) process, where the final photon is emitted either from the incoming or the outgoing leptons. At leading twist and leading order, the deeply virtual photon production cross section is composed of BH, DVCS, and interference terms. The amplitudes of the three terms can be approximated as a finite sum of Fourier harmonics, as shown for the nucleon in [38].

Due to limited statistics, we only bin our data two-dimensionally in the azimuthal angle (ϕ) and one of the kinemtical variables Q^2, x_B and t. Figure 4 presents A_{LU} for the three sets of binning. The asymmetries are fitted with the form of $\frac{\alpha sin(\phi)}{1+\beta cos(\phi)}$. Figure 5 shows the Q^2, x_B, and $-t$-dependencies of the fitted A_{LU} signals at $\phi = 90°$. The x_B and $-t$-dependencies are compared to theoretical calculations performed by S. Liuti and K. Taneja [41]. Their model relies on the impulse approximation and uses advanced spectral functions of nuclei. The calculations are at slightly different kinematics than our data but still provide some guidance. The experimental results appear to have larger asymmetries than the calculations. These differences may arise from nuclear effects which are not taken into account in the model, such as long-range interactions.

[1] D. Mueller, D. Robaschik, B. Geyer, F.M. Dittes and J. Horejsi, Fortsch. Phys. **42**, 101 (1994).
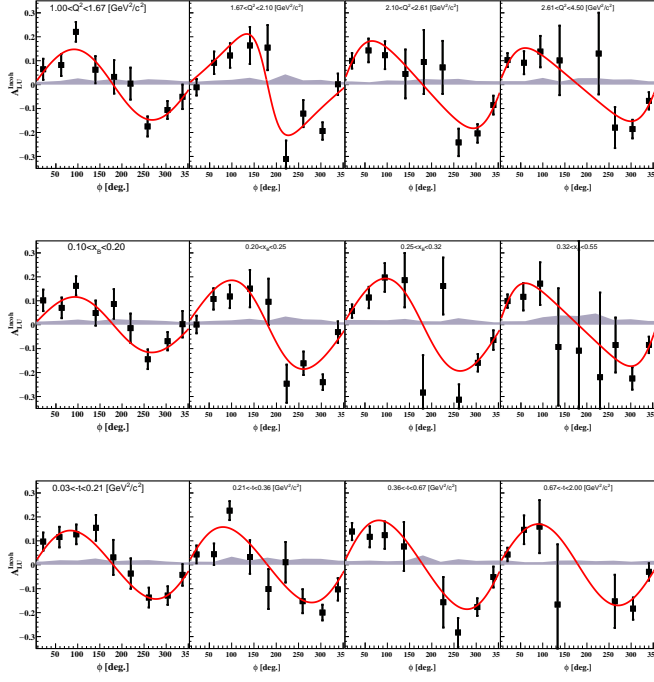
3

FIG. 4: The incoherent A_{LU} as a function of ϕ. Results are presented for different Q^2 bins (top panel), x_B bins (middle panel), and $-t$ bins (bottom panel). The error bars represent the statistical uncertainties. The gray bands represent the systematic uncertainties, including the normalisation uncertainties. The red curves are the results of our fits with the form $\frac{\alpha sin(\phi)}{1+\beta cos(\phi)}$.

FIG. 5: The Q^2 (left), x_B (middle), and $-t$-dependencies (right) of the A_{LU} at $\phi = 90°$ (black squares). On the middle plot: the full-red and the dashed-blue curves are theoretical calculations from [41]. On the right: the green circles are the HERMES $-A_{LU}$ (positron beam was used) inclusive measurements [?], the colored curves represent theoretical calculations from [41].

[2] X.D. Ji, Phys. Rev. Lett. **78**, 610 (1997).
[3] X.D. Ji, Phys. Rev. D **55**, 7114 (1997).
[4] A.V. Radyushkin, Phys. Lett. B **380**, 417 (1996).
[5] A.V. Radyushkin, Phys. Rev. D **56**, 5524 (1997).
[6] M. Burkardt, Phys. Rev. D **62**, 071503 (2000) Erratum: Phys. Rev. D **66**, 119903 (2002)
[7] M. Diehl, Eur. Phys. J. C **25**, 223 (2002) Erratum: Eur. Phys. J. C **31**, 277 (2003)
[8] A. V. Belitsky and D. Mueller, Nucl. Phys. A **711**, 118 (2002)
[9] M. Burkardt, Phys. Rev. D **72**, 094020 (2005)
[10] S. Stepanyan *et al.* [CLAS Collaboration], Phys. Rev. Lett. **87**, 182002 (2001).
[11] A. Airapetian *et al.* [HERMES Collaboration], Phys. Rev. Lett. **87**, 182001 (2001); JHEP **1207**, 032 (2012); JHEP **1006**, 019 (2010); JHEP **0806**, 066 (2008); Phys. Lett. B **704**, 15 (2011); Phys. Rev. D **75**, 011103 (2007); JHEP **0911**, 083 (2009); Phys. Rev. C **81**, 035202 (2010); JHEP **1210**, 042 (2012).
[12] S. Chekanov *et al.* [ZEUS Collaboration], Phys. Lett. B **573**, 46 (2003).
[13] A. Aktas *et al.* [H1 Collaboration], Eur. Phys. J. C **44**, 1 (2005).
[14] S. Chen *et al.* [CLAS Collaboration], Phys. Rev. Lett. **97**, 072002 (2006).
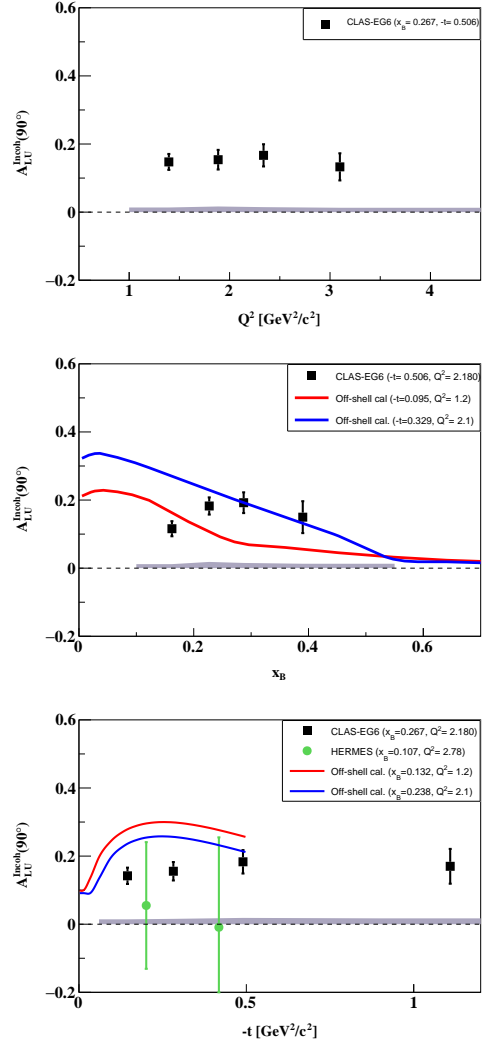[15] C. Muñoz Camacho *et al.* [Jefferson Lab Hall A Collaboration], Phys. Rev. Lett. **97**, 262002 (2006).
[16] F.X. Girod *et al.* [CLAS Collaboration], Phys. Rev. Lett. **100**, 162002 (2008).
[17] M. Mazouz *et al.* [Jefferson Lab Hall A Collaboration], Phys. Rev. Lett. **99**, 242501 (2007)
[18] G. Gavalian *et al.* [CLAS Collaboration], Phys. Rev. C **80**, 035206 (2009).
[19] E. Seder *et al.* [CLAS Collaboration], Phys. Rev. Lett. **114**, 032001 (2015).
[20] S. Pisano *et al.* [CLAS Collaboration], Phys. Rev. D **91**, 052014 (2015).
[21] H. S. Jo *et al.* [CLAS Collaboration], Phys. Rev. Lett. **115**, no. 21, 212003 (2015)
[22] K. Goeke, M.V. Polyakov and M. Vanderhaeghen, Prog. Part. Nucl. Phys. **47**, 401 (2001).
[23] M. Diehl, Phys. Rept. **388**, 41 (2003).

[24] X.D. Ji, Ann. Rev. Nucl. Part. Sci. **54**, 413 (2004).

[25] A.V. Belitsky and A.V. Radyushkin, Phys. Rept. **418**, 1 (2005).

[26] S. Boffi and B. Pasquini, Riv. Nuovo Cim. **30**, 387 (2007).

[27] M. Guidal, H. Moutarde and M. Vanderhaeghen, Rept. Prog. Phys. **76**, 066202 (2013).

[28] R. Dupré and S. Scopetta, Eur. Phys. J. A **52**, no. 6, 159 (2016)

[29] O. Hen, G. A. Miller, E. Piasetzky and L. B. Weinstein, arXiv:1611.09748 [nucl-ex].

[30] P. R. Norton, Rept. Prog. Phys. **66**, 1253 (2003).

[31] D. F. Geesaman, K. Saito and A. W. Thomas, Ann. Rev. Nucl. Part. Sci. **45**, 337 (1995).

[32] A. Freund and J.C. Collins, Phys. Rev. D **59**, 074009 (1998)

[33] X.-D. Ji and J. Osborne, Phys. Rev. D **58**, 094018 (1998)

[34] F. Ellinghaus *et al.* [HERMES Collaboration], AIP Conf. Proc. **675**, 303 (2003)

[35] V. Guzey and M. Strikman, Phys. Rev. C **68**, 015204 (2003)

[36] J. Seely *et al.* Phys. Rev. Lett. **103**, 202301 (2009)

[37] B. A. Mecking *et al.* [CLAS Collaboration], Nucl. Instrum. Meth. A **503**, 513 (2003).

[38] A. V. Belitsky, D. Mueller and A. Kirchner, Nucl. Phys. B **629**, 323 (2002)

[39] A. Kirchner and D. Mueller, Eur. Phys. J. C **32**, 347 (2003)

[40] A. V. Belitsky and D. Mueller, Phys. Rev. D **79**, 014017 (2009)

[41] S. Liuti and K. Taneja, Phys. Rev. C **72**, 032201 (2005)

[42] Private communications with V. Guzey based on: V. Guzey, Phys. Rev. C **78**, 025211 (2008).

[43] V. Guzey and T. Teckentrup, Phys. Rev. D **74**, 054027 (2006)

[44] Private communications with M. Guidal based on: M. Guidal, M. V. Polyakov, A. V. Radyushkin and M. Vanderhaeghen, Phys. Rev. D **72**, 054013 (2005).

[45] I. V. Musatov and A. V. Radyushkin, Phys. Rev. D **61**, 074027 (2000).

[46] Private communications with S. Liuti based on: J. O. Gonzalez-Hernandez, S. Liuti, G. R. Goldstein and K. Kathuria, Phys. Rev. C **88**, no. 6, 065206, (2013).